

PAPER • OPEN ACCESS

## Feasibility of radiosurgery dosimetry using NIPAM 3D dosimeters and x-ray CT

To cite this article: Justus Adamson *et al* 2019 *J. Phys.: Conf. Ser.* **1305** 012004

View the [article online](#) for updates and enhancements.

You may also like

- [Dose rate properties of NIPAM-based x-ray CT polymer gel dosimeters](#)  
A Jirasek, H Johnston and M Hilts
- [Thermosensitive and chitosan of crab \(\*Portunus pelagicus\*\) shells gel based adsorbent for reversible adsorption-desorption of several toxic metal ions](#)  
E O Ningrum, A Bagus, E Agustiani *et al.*
- [Multi-responsive fluorescent polymer microparticles in response to temperature, electricity and hydrogen oxide](#)  
Ran Li, Wei Nie and Wen Yang



**ECS**  
The  
Electrochemical  
Society  
Advancing solid state &  
electrochemical science & technology

**DISCOVER**  
how sustainability  
intersects with  
electrochemistry & solid  
state science research

# Feasibility of radiosurgery dosimetry using NIPAM 3D dosimeters and x-ray CT

Justus Adamson<sup>1</sup>, Jaelyn Carroll<sup>2</sup>, Michael Trager<sup>2</sup>, Paul Yoon<sup>2</sup>, Jacob Kodra<sup>2</sup>, Fang-Fang Yin<sup>1</sup>, Evan Maynard<sup>3</sup>, Michelle Hilts<sup>4</sup>, Mark Oldham<sup>1\*</sup> and Andrew Jirasik<sup>5\*</sup>

<sup>1</sup>Department of Radiation Oncology, Duke University Medical Center, Durham, North Carolina, USA

<sup>2</sup>Medical Physics Graduate Program, Duke University, Durham North Carolina, USA

<sup>3</sup>Department of Physics and Astronomy, University of Victoria, Victoria, BC, Canada

<sup>4</sup>Medical Physics, BC Cancer - Kelowna, BC, Canada

<sup>5</sup>Department of Physics, Irving K Barber School of Arts and Sciences, University of British Columbia – Okanagan Campus, Kelowna, BC, Canada

\*Equal contribution

E-Mail: justus.adamson@duke.edu

**Abstract.** We investigated the feasibility of using N-isopropylacrylamide (NIPAM) dosimeters with x-ray CT to verify radiosurgery dose. Dosimeters were prepared at one facility and shipped to a second facility for irradiation. A simulation CT was acquired and plans prepared for a 4 field box, and a 4 arc VMAT radiosurgery plan to 6 targets with 1cm diameter. Each dosimeter was aligned via CBCT and irradiated, followed by 5 diagnostic CTs acquired after >24 hours, which were averaged for analysis. Absolute dose calibration was applied and dose evaluated for both plans. Hounsfield Units were proportional to dose above 10-12Gy. For the 4-field box, mean difference between measured and predicted dose >10Gy was  $-0.13\text{Gy} \pm 1.69\text{Gy}$  and gamma index was <1 for 72% and 65% of voxels using a 5% / 1mm and 3% / 2mm criteria, respectively (threshold = 15Gy, global dose criteria). For the multifocal SRS case, mean dose within each target was within  $-0.14\text{Gy} \pm 0.55\text{Gy}$  of the expected value, and gamma index was < 1 for 94.0% and 99.5% of voxels, respectively (threshold = 15Gy). NIPAM based 3D dosimetry with x-ray CT is well suited for validating radiosurgery spatial alignment, as well as dose distributions when dose is above 10-12Gy.

## 1. Introduction

Single isocenter volumetric-modulated arc therapy (VMAT) has recently been applied for radiosurgery of multifocal intracranial disease [1,2]. This technique has many advantages, but also requires increased attention to spatial accuracy especially for rotational errors, as small targets may be located at a distance from the isocenter [2-4]. Another major challenge is the difficulty in verifying the complex dose distribution. The radiosurgery plans include high dose gradients and dispersed small target volumes which are often similar or smaller in size than the detector spacing of many of the technologies used for typical VMAT verification. Film measurements provide high spatial resolution, but are limited to a single plane and require additional effort for digitization. A number of specialized digital detectors exist for verifying dose planes at sufficiently high resolution for radiosurgery, but for smaller field sizes than those encountered in multifocal radiosurgery [5].



3D dosimetry systems have unique advantages for these special circumstances, in that they can offer comprehensive dosimetric measurements at high spatial resolution [6-9]. Despite potential advantages, 3D dosimetry is challenged by the limited access to optical CT or MRI for reading out dose information, and lack of specialized commercial analysis [10]. Alternatively, for some 3D dosimeter materials such as N-isopropylacrylamide (NIPAM) [11,12], radiation dose invokes a change in mass density which can be read out as change in Hounsfield Unit in x-ray CT [13]. To date, there has been much previous research which has included increasing the sensitivity of dosimeter materials [14,15], and improving the dose readout through selective CT acquisition and reconstruction parameters [16], and post processing [17,18]. Despite these improvements, the main limitation to x-ray CT 3D dosimetry is still the limited dose sensitivity due to the small size of density changes (approximately  $1 \text{ mg/cm}^3$  per 1 Gy of absorbed dose) [19], however this becomes much less problematic in the setting of high dose and high dose gradients for radiosurgery.

In this study, we investigate the feasibility of using a NIPAM dosimeter with x-ray CT for verification of radiosurgery.

## 2. Materials and Methods

Two NIPAM dosimeters and one “blank” dosimeter without the active agents were prepared at one facility (Department of Physics and Astronomy, University of Victoria, Victoria, BC, Canada). Each dosimeter was poured into a cylindrical plastic jar with a 9.5cm diameter and 15.3cm height. The dosimeters were then shipped commercially to a second facility (Department of Radiation Oncology, Duke University, Durham NC, USA) for irradiation, being packaged in an insulated box with dry ice, thus remaining at a refrigerated temperature. The dosimeters arrived at the second facility after 2 days, after which they were stored in a refrigerator at all times except during the X-ray CTs and irradiation. The subsequent treatment planning and irradiation were performed on the same day that the dosimeters arrived.

### 2.1. Treatment Planning & Delivery

*2.1.1. General Details.* For this example, simulation CTs of each dosimeter were acquired for treatment planning; fiducials were placed on the superior portion of the dosimeter to allow for reproducible setup. Treatment plans were prepared within the Varian External Beam Treatment Planning software version 13.6 (Varian Medical Systems) with the Anisotropic Analytical Algorithm (version 13.6.23). We utilized a Truebeam STX linear accelerator with 6MV photons and HD-MLCs.

The first dosimeter received a treatment plan in which the top half included a 3-field irradiation pattern used for the absolute dose calibration, which has been described in detail previously [12]. The plan utilizes three rectangular (3cmx7cm) fields at oblique angles, designed so that the high dose area includes a range of dose values to aid in the absolute dose calibration. For this case, the prescribed dose was 20Gy, delivered in a single irradiation with 6MV photons, with a maximum dose of 27.0Gy. The lower half of the first dosimeter included a simple 4-field box irradiation, which served as a simple evaluation of the feasibility of using the NIPAM dosimeter for remote dosimetry, and as an example of the possibility of including the calibration and test dosimetry in the same dosimeter. The 6MV photon 4-field box also consisted of a 20Gy irradiation with open fields of size 5cm square; the maximum planned dose of the 4 field box was 25.0Gy.

A single isocenter multifocal VMAT SRS plan was prepared for the 2<sup>nd</sup> dosimeter with 6 targets, each with a 1cm diameter. The SRS plan utilized 4 non-coplanar VMAT arcs with a 6MV photon beam; the treatment planning technique has been described previously [20,21]. Each target was prescribed a dose of 20Gy, with the maximum dose being 31.3Gy.

## 2.2. Analysis

To minimize statistical noise, we created an average CT image for each of the NIPAM dosimeters (blank, calibration, and SRS test), which consisted of the average of all 5 individual image series. The calibration and SRS test dosimeters were processed including subtracting the background image (from the average CT of the blank dosimeter). The CT image of the dosimeters was registered to the treatment planning dose matrix, and the planning dose matrix was re-sampled to match the resolution of the dosimeter CT image. A calibration curve was created to convert Hounsfield Units from the dosimeter after background subtraction,  $h$ , to dose,  $d$ , using the fit:

$$d = d_0 + a_1(h - a_2)^{a_3} \quad (1)$$

where  $d_0$  is the cutoff dose below which the Hounsfield Units within the dosimeter are not above the background signal, and  $a_1$ ,  $a_2$ , and  $a_3$  are variables that are fit through an iterative optimization process via in-house code in Matlab (Mathworks, Natick, MA). For this analysis,  $d_0$  was set to 10Gy, as Hounsfield Units below this dose level were not above the background signal. The iterative optimization yielded values of  $a_1$ ,  $a_2$ , and  $a_3$  of 0.850 Gy/HU, -20.160 HU, and 0.978 (no units), respectively. This fit was then used to convert Hounsfield Units to dose for the SRS test dosimeter.

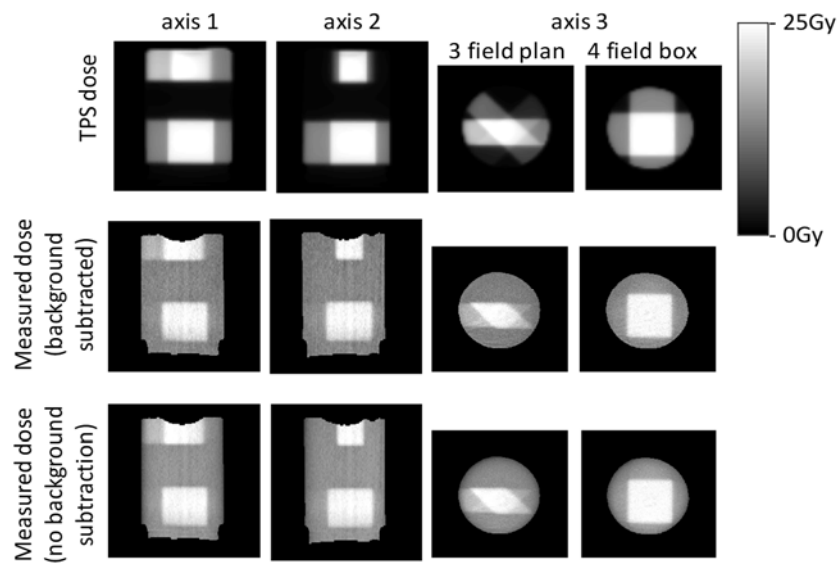
The SRS test dosimeter dose was then compared to the treatment planning system dose within Matlab, including gamma index analysis, dose profiles, and isodose comparisons. Gamma analysis was performed using various criteria with a lower dose threshold of 30% of the maximum dose in order to eliminate noise from the dosimeter and low dose regions.

## 3. Results

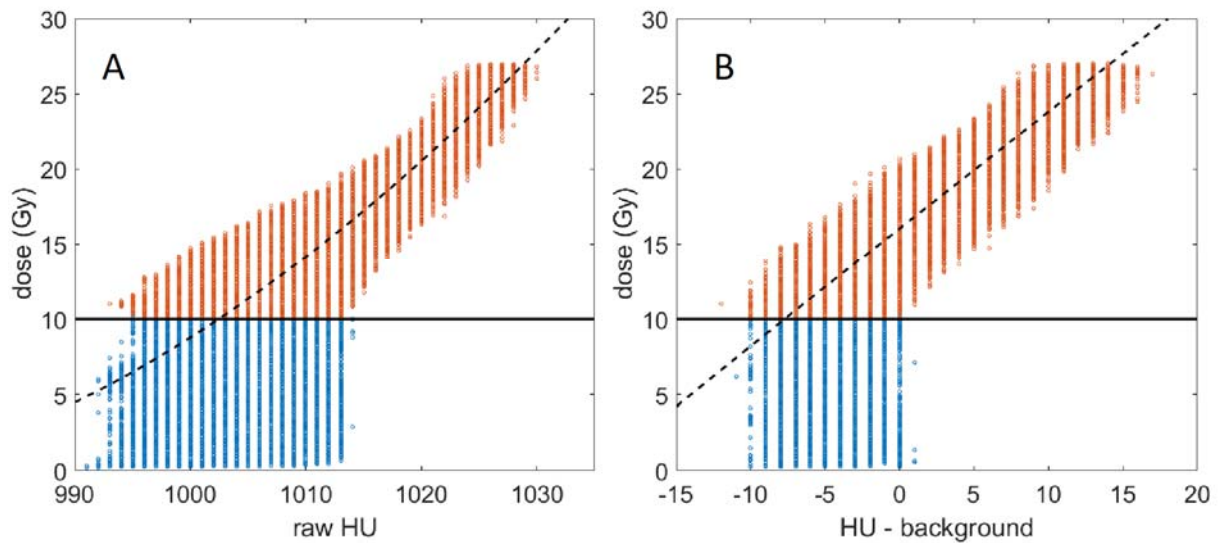
The planned and measured dose distribution (both when with and without subtracting the background signal) for the entire first dosimeter is shown in Figure 1. As is visible in Figure 1, while the dosimeter yielded a signal that was proportional to dose in the high dose areas (above 10Gy), this proportionality was non linear and had poor dose sensitivity for lower values. This was also the case for the second dosimeter below a threshold of around 12Gy. After fitting the HU values and dose distribution from the 3 field plan, the fit values from equation 1 to convert HU after subtracting the background signal to absolute dose was  $a_1=0.850$  Gy / HU,  $a_2=-20.160$  HU, and  $a_3=0.978$ . When the background was not subtracted, the fit values were  $a_1=0.027$  Gy / HU,  $a_2=969.477$  HU, and  $a_3=1.6881$ . For both cases the threshold dose  $d_0$  below which voxels were excluded from the analysis was 10Gy. The scatter plot of HU and dose with and without subtracting the background signal, along with the dose fit from Equation 1 is shown in Figure 2(a) and 2(b).

Figure 3 shows dose profiles intersecting the four-field box plan. For this plan, the overall difference (mean  $\pm$  standard deviation) between measured and predicted dose for all dose values above 10Gy was  $-0.20\text{Gy} \pm 1.72\text{Gy}$  and  $-0.13\text{Gy} \pm 1.69\text{Gy}$  with and without the background signal subtracted, respectively. The gamma index over the 4 field dose plan was less than 1 for 72% and 65% of voxels when using a 5% / 1mm and 3% / 2mm criteria, respectively (threshold = 15Gy, using a global dose criteria).

Figure 4 shows the dose distribution for the TPS and measurement from the SRS plan. The mean dose per target was within  $-0.14\text{Gy} \pm 0.54\text{Gy}$  of the expected value from the TPS. The gamma index over the entire dosimeter was less than 1 for 94.0% and 99.5% of voxels when using a 5% / 1mm and 3% / 2mm criteria, respectively (threshold = 15Gy, using a global dose criteria).



**Figure 1.** Planned and measured dose distribution for 3 and 4 field treatment plans after applying absolute dose calibration.



**Figure 2.** Relationship between dose and Hounsfield Unit for absolute dose calibration portion of the dosimeter after subtracting background (a) and using raw Hounsfield Units (b). Points excluded from the fit are shown below the 10Gy threshold line.

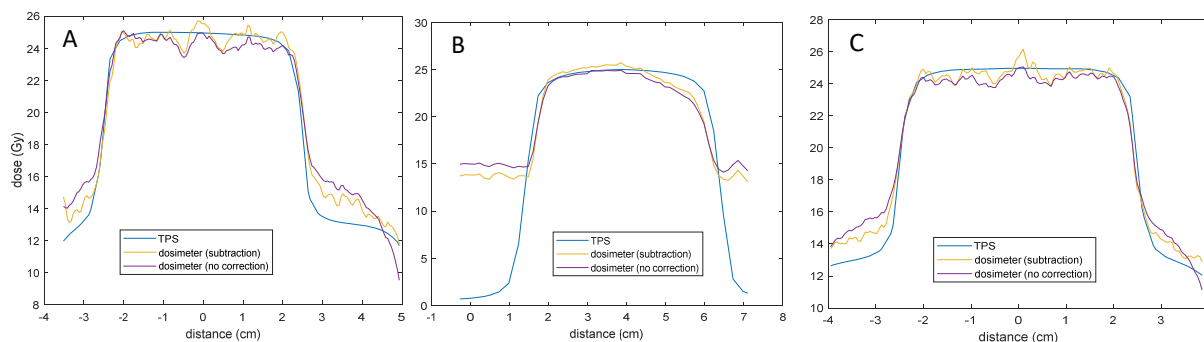


**Figure 3.** Planned and measured dose profiles across the 4-field box for each axis.

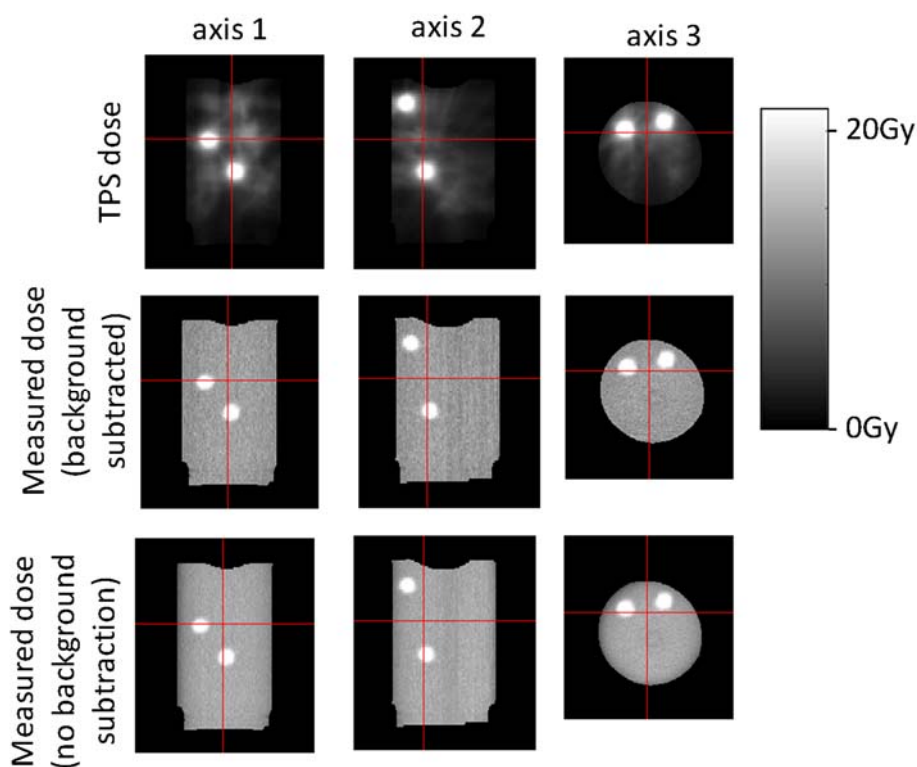


**Figure 4.** Planned and measured dose distributions for the SRS irradiation.

#### 4. Discussion and Conclusion

In this study we used a polynomial fit of dose values above 10-12Gy. Earlier studies used an S-shaped dose calibration curve which has included these lower dose values; in this study, we used a simpler polynomial fit which excludes the area of lower sensitivity but allows for easier conversion back to dose. We anticipate that using a greater number of averaged CT scans would increase this sensitivity and allow for better dose resolution in the lower dose range. This represents a proof of principle of the ability to verify accurate alignment of the radiotherapy dose immediately after irradiation using a NIPAM dosimeter with x-ray CT. High dose areas (greater than 10-12Gy) were well correlated with expected dose.

#### 5. References

- [1] Clark G M *et al* 2010 *Int. J. Radiat. Oncol. Biol. Phys.* **76** 296-302

- [2] Stanhope C *et al* 2016 *Pract. Radiat. Oncol.* **6** 207-213
- [3] Roper J *et al* 2015 *Int. J. Radiat. Oncol.* **93** 540-6
- [4] Faught A M *et al* 2016 *Med. Phys.* **43** 5437
- [5] Sarkar V *et al* 2016 *J. Radiosurgery* **4** 213-23
- [6] Sakhalkar H S *et al* 2009 *Med. Phys.* **36** 71-82
- [7] Hurley C *et al* 2006 *Nucl. Instrum. Meth. A* **565** 801-11
- [8] Mather M L *et al* 2003 *Phys. Med. Biol.* **48** N269-75
- [9] Baldock C 2009 *J. Phys.: Conf. Ser.* **164** 012002
- [10] Rowshanfarzad P *et al* 2011 *J. Appl. Clin. Med. Phys.* **12** 3645
- [11] Johnston H *et al* 2012 *Phys. Med. Biol.* **57** 3155-75
- [12] Jirasek A *et al* 2017 *Med. Phys.* 736-46
- [13] Hilts M *et al* 2000 *Phys. Med. Biol.* **45** 2559-71
- [14] Chain J N M *et al* 2011 *Phys. Med. Biol.* **56** 2091-102
- [15] Jirasek A *et al* 2010 *Phys. Med. Biol.* **55** 5269-81
- [16] Hilts M *et al* 2005 *Phys. Med. Biol.* **50** 1727-45
- [17] Hilts M and Jirasek A 2008 *Med. Phys.* **35** 344-55
- [18] Jirasek A *et al* 2012 *Phys. Med. Biol.* **57** 3137-53
- [19] Baldock C *et al* 2010 *Phys. Med. Biol.* **55** R1-63
- [20] Stanhope C *et al* 2016 *Pract. Radiat. Oncol.* **6** 207-13
- [21] Morrison J *et al* 2016 *Med. Dosim.* **41** 285-9